# Interplay of spin glass physics and the Kondo effect in a model for dilute magnetic alloys

Farhad Fazileh and Eugene H. Kim

*Department of Physics, University of Windsor, Windsor, Ontario, Canada N9B 3P4*

The interplay of spin glass physics and the Kondo effect is discussed for a model of dilute magnetic alloys. The physics is analyzed in terms of the distribution of internal magnetic fields. Using this approach, we determine the phase diagram of the model; we determine the properties of the model in the phases with broken ergodicity.

## I. INTRODUCTION

The problem of magnetic impurities in metals has been of considerable interest for some time.[1,2] Magnetic impurities cause spin-flip scattering of the conduction electrons; they give rise to the Kondo effect[3] with its dynamically generated scale, the Kondo temperature $T_K$. The physics behind this dynamically generated scale is a correlated many-body state, where the impurity spin is locked in a singlet with a cloud of electrons—the Kondo screening cloud.[1] The Kondo temperature reflects the size of the screening cloud. In addition to the Kondo effect, the conduction electrons mediate an effective interimpurity interaction—the Ruderman-Kittel-Kasuya-Yosida (RKKY) interaction;[4] as the impurities are in random positions, it is a random interimpurity interaction. In magnetic alloys, the RKKY interaction can give rise to ferromagnetism; it can also give rise to a spin glass phase having many metastable states.[2]

Recently, the resistivity $\rho(T)$ of gold wires doped with very dilute amounts of iron was measured; signs of both the Kondo effect and spin glass physics were observed in $\rho(T)$.[5] In these systems, the concentration of iron was more dilute than in alloys where spin glass physics was observed previously; in describing these systems, a proper treatment of both the Kondo effect as well as spin glass physics is necessary. Motivated by these experiments, in this work we consider a model to understand the properties of very dilute magnetic alloys and, in particular, the effects of coherence between partially screened impurities.

The rest of this paper is organized as follows. In Sec. II, we describe the model considered in this work and the approach employed to treat the model. Rather than use the replica formalism which is typically used to treat spin glasses[2] and which has been used in previous works studying the interplay of random interimpurity interactions and the Kondo effect,[6,7] in this work we employ an approach motivated by the seminal work of Ref. 8. More specifically, rather than average over the random interimpurity interaction in the beginning (which one does in the replica formalism), we treat one configuration of random interimpurity interactions at a time and perform the average over the random interimpurity interactions in the end. In Sec. III, we consider the physics via an Ansatz for the distribution of fields, which is equivalent to a "replica-symmetric ansatz" within the replica formalism. Using this ansatz, we determine the phase diagram of the model considered in this work. In Sec. IV we

discuss the physics within the phases with broken ergodicity; in particular, we present results for the distribution of internal fields. By necessity, our analysis in this section is primarily numerical. Previous works studying the interplay of Kondo physics and random impurity interactions focussed on the "replica-symmetric" phase(s);[6,7] the properties of the glass phase itself were not discussed. Section V presents some concluding remarks and possibilities for future work.

## II. THE MODEL AND APPROACH

We begin with a model of conduction electrons interacting with a dilute collection of randomly placed magnetic impurities $H = H_0 + H_{sd}$, where $H_0$ is the free Hamiltonian of the conduction electrons and

$$H_{sd} = \sum_i J_0 \tau \cdot \mathbf{S}(\mathbf{r}_i). \tag{1}$$

In Eq. (1), $\tau_i$ is the spin operator of the $i$th magnetic impurity (located at $\mathbf{r}_i$); $\mathbf{S}(\mathbf{r}_i)$ is the conduction electrons' spin operator at $\mathbf{r}_i$; $J_0$ describes the coupling between the conduction electrons and the magnetic impurities. In this work, we focus on the case of spin-1/2 impurities; we take the interaction between the conduction electrons and the magnetic impurities to be antiferromagnetic $J_0 > 0$.

To make progress, we integrate out high-energy conduction electrons; we focus our attention on the conduction electrons' degrees of freedom with wavelengths much larger than the distance between impurties. More specifically, we integrate out conduction electrons in the regime $D' < E < D$, where $D$ is half the conduction electrons' bandwidth, and $D'$ is an energy satisfying $D' \ll v_F/R$ ($v_F$ is the Fermi velocity; $R$ is the average distance between impurities.) Upon doing this, an effective interimpurity interaction—the RKKY interaction—is generated.[9] Therefore, to describe the system for $E < D'$, we have the effective Hamiltonian

$$H = H_0 + H_{imp}, \tag{2}$$

where $H_{imp} = H_{sd} + H_{RKKY}$ with

$$H_{sd} = \sum_i \{ J^{xy} [\tau_i^+ S^-(\mathbf{r}_i) + \text{H.c.}] + J^z \tau_i^z S^z(\mathbf{r}_i) \}, \tag{3a}$$

$$H_{\text{RKKY}} = -\frac{1}{2} \sum_{i \neq j} K_{i,j} \tau_i^z \tau_j^z. \tag{3b}$$

Equation (2) is the Hamiltonian we analyze in this work to understand the physics occurring at distances sufficiently larger than the interimpurity spacing—it is the Hamiltonian we employ to understand the interplay of spin glass physics and the Kondo effect in dilute magnetic alloys. As before, $H_0$ in Eq. (2) is the free Hamiltonian of the conduction electrons; now, however, we consider only those degrees of freedom in a regime about the Fermi energy with $E < D'$ (as the higher energy degrees of freedom have been integrated out.) As before, Eq. (3a) describes the interaction between the conduction electrons and the magnetic impurities, and is responsible for the Kondo effect. The parameters $\{J^{xy}, J^z\}$ in Eq. (3a) are to be understood as renormalized parameters (from integrating out the high-energy conduction electrons). Note that we will consider an anisotropic interaction $J^{xy} \neq J^z$ in what follows. It is known that the Hamiltonian with $J^{xy} \neq J^z$ has the same low energy physics as the isotropic limit $J^{xy} = J^z$.[1] Finally, Eq. (3b) is the effective interimpurity interaction that was generated upon integrating out the high-energy conduction electrons; $\{K_{i,j}\}$ are the (random) interimpurity couplings. To simplify the analysis in what follows, we have taken the interimpurity interaction to be an Ising interaction. Physically, such an interaction could arise due to crystal field effects; it is relevant to magnetic alloys such as ZnMn and AgMn.[2]

To analyze Eq. (2), we treat the interimpurity interaction in mean-field theory. This approach, which is motivated by the seminal work of Ref. 8, has recently been used to study the transverse field Ising glass.[11] This approach is valid to describe the finite temperature properties within the glass phase. It is not expected to describe the properties at $T=0$ or the critical behavior at a phase transition, as fluctuations are ignored. In this approximation, $H_{\text{imp}} \simeq \Sigma_{i=1}^N H_{\text{imp}}^i$, where

$$H_{\text{imp}}^i = J^{xy}[\tau_i^+ S^-(\mathbf{r}_i) + \tau_i^- S^+(\mathbf{r}_i)] + J^z \tau_i^z S^z(\mathbf{r}_i) - h_i \tau_i^z, \tag{4}$$

where

$$h_i = \sum_j K_{i,j} \langle \tau_j^z \rangle \tag{5}$$

being an effective, random field acting on impurity $i$ due to the rest of the impurities. The $\{\langle \tau_j^z \rangle\}$ are to be determined self-consistently. As the fields $\{h_i\}$ are random, physical quantities must be averaged over the distribution of fields

$$\mathcal{P}(h_i) = \left\langle \delta\left(h_i - \sum_j K_{i,j} \langle \tau_j^z \rangle\right) \right\rangle_{K_{i,j}}, \tag{6}$$

where $\langle \cdots \rangle_{K_{i,j}}$ denotes averaging over the distribution of couplings $K_{i,j}$. Note that information about the various phases which arise is contained in $\mathcal{P}(h_i)$.

To proceed further, we expand the conduction electron operator in spherical waves centered about each impurity. Furthermore, we approximate by ignoring the overlap between conduction electron wave functions centered about different impurities. This approximation is justified, provided the concentration of impurities is sufficiently dilute and the distances between impurities are large—the effects ignored are subleading, being suppressed by powers of $(k_F R)$.[9] ($k_F$ is the Fermi wave vector.) In this approximation, each impurity is coupled to its own bath of conduction electrons. As we are taking the interaction between the conduction electrons and the impurity to occur at a point [see Eq. (4)], only a single harmonic—namely, the $s$-wave channel—couples to the impurity.[10] Focussing on this $s$-wave channel, we can write an effective one-dimensional model for the conduction electron bath centered about each impurity. Our Hamiltonian becomes $H = \Sigma_{i=1}^N H_i$, where $H_i = H_0^i + H_{\text{imp}}^i$ with

$$H_0^i = -iv_F \int dx \, \psi_{R,i,s}^\dagger \partial_x \psi_{R,i,s} + \cdots, \tag{7}$$

$$H_{\text{imp}}^i = 2\pi v_F \lambda^{xy} [\tau_i^+ J_{R,i}^-(0) + \tau_i^- J_{R,i}^+(0)] + 2\pi v_F \lambda^z \tau_i^z J_{R,i}^z(0)$$
$$+ h_i \tau_i^z. \tag{8}$$

In Eq. (7), $\psi_{R,i,s}$ destroys a (right-moving) electron with spin-$s$ in the bath centered about the $i$th impurity, $v_F$ is the Fermi velocity, the ellipses represent higher harmonics, which do not couple to the magnetic impurities. In Eq. (8),

$$J_{R,i}^\alpha(0) = (1/2) \psi_{R,i,s}^\dagger(0) \sigma_{s,s'}^\alpha \psi_{R,i,s'}(0),$$

with $\{\sigma_{s,s'}^\alpha\}$ ($\alpha = x, y, z$) being the Pauli matrices; $\lambda^{xy} = J^{xy} \rho_0$ and $\lambda^z = J^z \rho_0$ are dimensionless couplings ($\rho_0$ is the conduction electrons' density-of-states).

In what follows, it will prove useful to utilize the boson representation of one-dimensional fermions.[12] To do so, the electron operator is written as

$$\psi_{R,i,s} \sim \frac{1}{\sqrt{2\pi\alpha}} \exp(i\sqrt{4\pi} \phi_{R,i,s}),$$

where $\phi_{R,i,s}$ is a chiral Bose field, and $\alpha$ is a short-distance cutoff ($\alpha \simeq v_F/D'$). It will also prove useful to form charge and spin fields $\phi_{R,i,\rho/\sigma} = (\phi_{R,i,\uparrow} \pm \phi_{R,i,\downarrow})/\sqrt{2}$. In terms of these variables,

$$H_i = v_F \int dx (\partial_x \phi_{R,i,\sigma})^2 + (\partial_x \phi_{R,i,\rho})^2 + \frac{v_F \lambda^{xy}}{\alpha} [\tau_i^+ e^{-i\sqrt{8\pi}\phi_{R,i,\sigma}(0)}$$
$$+ \tau_i^- e^{i\sqrt{8\pi}\phi_{R,i,\sigma}(0)}] + v_F \lambda^z \sqrt{2\pi} \tau_i^z \partial_x \phi_{R,i,\sigma}(0) + h_i \tau_i^z. \tag{9}$$

Notice that only the spin fields couple to the magnetic impurities; the charge fields decouple.

From Eq. (9) along with Eq. (6), we can readily understand the properties of the system and, in particular, how they are affected by Kondo physics. To treat the Kondo effect nonperturbatively, we perform a unitary transformation

$$U = \exp[i\beta \tau^z \phi_{R,i,\sigma}(0)]$$

with $\beta = \sqrt{\pi}(\sqrt{2} - 1)$, which ties (part of) the conduction electrons' spin to the impurity.[12] Then, we introduce new fermion fields, $d_i \sim \tau_i^-$, and $\tilde{\psi}_{R,i} \sim e^{i\sqrt{4\pi}\phi_{R,i,\sigma}}$. Upon performing these transformations, $H_i$ becomes

$$H_i = v_F \int dx (\partial_x \phi_{R,i,\rho})^2 - i v_F \int dx \, \tilde{\psi}^\dagger_{R,i} \partial_x \tilde{\psi}_{R,i}$$

$$+ v_F \lambda^{xy} \sqrt{\frac{2\pi}{\alpha}} [d^\dagger_i \tilde{\psi}_{R,i}(0) + \tilde{\psi}^\dagger_{R,i}(0) d_i] + h_i \left( d^\dagger_i d_i - \frac{1}{2} \right)$$

$$+ v_F \sqrt{2\pi} \left[ \lambda^z - \left( 1 - \frac{1}{\sqrt{2}} \right) \right] \left( d^\dagger_i d_i - \frac{1}{2} \right) \tilde{\psi}^\dagger_{R,i}(0) \tilde{\psi}_{R,i}(0). \tag{10}$$

For the remainder of this work, we will focus on the Toulouse point, $\lambda^z = 1 - 1/\sqrt{2}$. The Toulouse point is known to have the same low-energy fixed point as the SU(2) symmetric Kondo model. However, the analysis simplifies at this point in parameter space—the marginally relevant operator near the ultraviolet fixed point (responsible for the Kondo logarithms) is fine-tuned away; similarly, the leading irrelevant operator near the infrared fixed point is also fine-tuned away.[12]

Up to now, our discussion was quite general; in order to proceed further, an explicit form of the interimpurity interaction is needed. To be able to make further progress analytically, we take the $\{K_{i,j}\}$ to be infinite ranged with a Gaussian distributed interaction between pairs of impurities as in the Sherrington-Kirkpatrick (SK) model[13]

$$\mathcal{P}(K_{i,j}) = \sqrt{\frac{N}{2\pi K^2}} \exp \left[ -\frac{N}{2K^2} (K_{i,j} - K_0/N)^2 \right]. \tag{11}$$

In Eq. (11), we have formally allowed for ferromagnetic ordering via $K_0$. (For the systems we are interested in and for which our approach is intended to describe, the density of magnetic impurities is too low to expect ferromagnetic ordering. However, it is interesting to formally consider the influence of ferromagnetic ordering within the context of this model.) While actual spin glass materials have interactions which are finite ranged, the results obtained from this infinite-ranged model are useful for understanding finite-ranged spin glass models and, hence, actual spin glass materials. Both finite- and infinite-ranged models have a complex free energy landscape with many metastable states; the phases that appear in the infinite-ranged model also arise in finite-ranged models. [The distribution of internal fields $\mathcal{P}(h_i)$ has the same qualitative behavior in the various phases in both models.[14,15]] A key difference, however, between the finite- and infinite-ranged models is that the infinite-ranged model has broken ergodicity, while finite-ranged models are believed not to.[16] However, the same relaxation phenomena that happens among metastable solutions in the infinite-ranged model (within a particular broken ergodicity phase) is expected to occur among metastable states in short-ranged models.[2] Hence, the salient features of our results are expected to be relevant to actual spin glass materials.

The Hamiltonian of Eq. (2) with $\mathcal{P}(K_{i,j})$ given by Eq. (11) has been considered in other works. In addition to being relevant to metals doped with magnetic impurities, this physics is also relevant to heavy fermion materials[6] and possibly high-temperature superconductors.[7] More generally, it has potential relevance to systems having both magnetic mo-

ments and itinerant electrons. In other treatments, the replica formalism was used. Furthermore, these works considered primarily a replica symmetric ansatz for the order parameter; properties of the spin glass phase itself were not discussed. Here we present a description of the various phases, including the phases with broken ergodicity, in terms of the distribution of internal fields [Eq. (6)].

### III. GAUSSIAN FIELD DISTRIBUTION

We now analyze the physics contained in our model. In this section, we treat the impurity spins in the simplest approximation—we take them to be uncorrelated and independent of the $\{K_{i,j}\}$; this gives rise to a Gaussian distribution of internal fields. We use this distribution of internal fields to determine the phase diagram of the model. The approach presented in this section is equivalent to a "replica symmetric ansatz" when the replica formalism is used. This is because the physics underlying the replica symmetric ansatz and the Gaussian distribution of internal fields is the same—correlations between different impurity spins are ignored.

#### A. Distribution of fields and mean-field variables

We begin by computing the distribution of fields $\mathcal{P}(h_i)$. To do so, we use a Fourier representation of the delta function; then Eq. (6) becomes

$$\mathcal{P}(h_i) = \int \frac{d\lambda}{2\pi} \prod_{j=1}^{N} \sqrt{\frac{N}{2\pi K^2}} \int dK_{i,j}$$

$$\times \exp \left[ -\frac{N}{2K^2} (K_{i,j} - K_0/N)^2 + i\lambda \left( h_i - \sum_j K_{i,j} \langle \tau^z_j \rangle \right) \right].$$

If we assume $\langle \tau^z_j \rangle$ to be uncorrelated between different sites and independent of the $\{K_{i,j}\}$, the intergrals can be readily carried out. Indeed, performing the integrals over the $\{K_{i,j}\}$ and then the integral over $\lambda$, we obtain[17]

$$\mathcal{P}(h_i) = \frac{1}{\sqrt{2\pi K^2 q}} \exp[-(h_i - K_0 m)^2/(2K^2 q)]. \tag{12}$$

In Eq. (12) $m \equiv \overline{\langle \tau^z_i \rangle}$ and $q \equiv \overline{\langle \tau^z_i \rangle^2}$, where the overline denotes averaging with respect Eq. (12) itself. This assumption of $\langle \tau^z_j \rangle$ being uncorrelated between different sites and independent of the $\{K_{i,j}\}$ is equivalent to a replica-symmetric ansatz using the replica formalism.[17] As is well known, this assumption breaks down at low temperatures; the resulting phase is one with broken ergodicity and many metastable states. The breakdown of Eq. (12) and the resulting phase(s) will be discussed below.

Using Eq. (10), we can readily understand the properties of the phases described by the field distribution in Eq. (12). To do so, we begin by determining $m$ and $q$ self-consistently. Computing $\langle \tau^z_i \rangle$, we find

$$\langle \tau^z_i \rangle = \frac{1}{\pi} \text{Im} \left[ \psi \left( \frac{1}{2} + \frac{T_k}{4\pi T} + i \frac{h_i}{2\pi T} \right) \right], \tag{13}$$

where $\psi(z)$ is the digamma function,[18] and $T_K = 2\pi v_F (\lambda^{xy})^2/\alpha$ is the Kondo temperature at the Toulouse

point. Using Eq. (13) and averaging over the internal fields with Eq. (12), we obtain

$$m = \int \frac{dy}{\sqrt{2\pi}} \exp(-y^2/2) \frac{1}{\pi} \text{Im}[\psi(z)], \qquad (14a)$$

$$q = \int \frac{dy}{\sqrt{2\pi}} \exp(-y^2/2) \frac{1}{\pi^2} (\text{Im}[\psi(z)])^2, \qquad (14b)$$

where

$$z = \left(\frac{1}{2} + \frac{T_K}{4\pi T}\right) + \frac{i}{2\pi T}(K\sqrt{q}y + K_0 m). \qquad (15)$$

It is worth noting that if we ignore the Kondo effect, i.e., if we consider $T_K \to 0$,[18]

$$\lim_{T_K \to 0} \text{Im}[\psi(z)] = \pi \tanh[\beta(yK\sqrt{q} + K_0 m)]$$

($\beta = 1/T$). Hence, Eqs. (14a) and (14b) reduce to the self-consistent equations determining $m$ and $q$ in the SK model.[13]

## B. Almeida-Thouless instability

Now we consider the stability of the phases described by Eq. (12). More specifically, we consider the occurrence of the Almeida-Thouless instability,[19] which marks the transition to a state with broken ergodicity. To this end, we consider the spin glass susceptibility

$$\chi_{\text{SG}} = \frac{1}{N} \sum_{i,j} \langle [\chi_{i,j}(i\omega_m \to 0)]^2 \rangle_{K_{i,j}},$$

where

$$\chi_{i,j}(i\omega_m) = -\langle T \tau_i^z(\tau) \tau_j^z \rangle(i\omega_m)$$

is the Matsubara representation of the imaginary time spin correlation function; as before, $\langle \cdots \rangle_{K_{i,j}}$ denotes averaging over the distribution of $\{K_{i,j}\}$. Since we are considering an infinite ranged model, $\chi_{\text{SG}}$ is given by ladder diagrams of the type shown in Fig. 1;[20,21] we obtain

$$\chi_{\text{SG}} = \frac{\overline{[\chi_i^0(i\omega_m \to 0)]^2}}{1 - K^2 \overline{[\chi_i^0(i\omega_m \to 0)]^2}}, \qquad (16)$$

where

$$\chi_i^0(i\omega_m \to 0) = \frac{1}{2\pi^2 T} \text{Re}\left[\psi'\left(\frac{1}{2} + \frac{T_K}{4\pi T} + i\frac{h_i}{2\pi T}\right)\right]$$

with $\psi'(z)$ being the trigamma function,[18] and the overline denotes averaging with respect to the field distribution, Eq. (12).

The phases described by the field distribution in Eq. (12) are stable provided $\chi_{\text{SG}} > 0$. More explicitly, we must have

$$1 > (\beta K)^2 \int \frac{dy}{\sqrt{2\pi}} \exp(-y^2/2) \frac{1}{4\pi^4} \{\text{Re}[\psi'(z)]\}^2, \quad (17)$$

where $z$ is given by Eq. (15). Note that if we ignore the Kondo effect $T_K \to 0$ (Ref. 18)
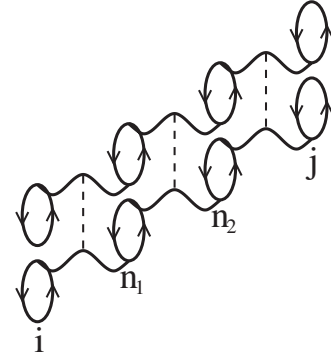


FIG. 1. Diagram contributing to the spin glass susceptibility. Solid lines denote impurity fermion propagators, wavy lines denote the interimpurity interaction $K_{i,j}$, dashed lines denote averaging over the distribution of $\{K_{i,j}\}$. The fermion particle-hole bubbles are averaged over the distribution of fields Eq. (12).

$$\lim_{T_K \to 0} \text{Re}[\psi'(z)] = 2\pi^2 \text{sech}^4[\beta(yK\sqrt{q} + K_0 m)]$$

($\beta = 1/T$). Hence, Eq. (17) reduces to the equation determining the AT instability in the SK model.[19] By definition/construction, $\chi_{\text{SG}}$ is a positive-definite quantity. $\chi_{\text{SG}}$ becoming negative tells us that our assumption leading to Eq. (12)—the assumption that the internal fields at different sites are uncorrelated—breaks down. The resulting phase is one with broken ergodicity; the distribution of internal fields in this phase is not described by Eq. (12).[2]

It is worth noting that the criterion in Eq. (17) for the instability to a phase with broken ergodicity would also be obtained if the replica formalism were used (albeit with considerably more difficulty).[2,20,21] More specifically, the criterion in Eq. (17) is obtained in the replica formalism by considering Gaussian fluctuations about the replica symmetric ansatz.[19] The same criterion [Eq. (17)] arises in two (seemingly) different approaches because the assumptions behind the replica symmetric ansatz and the field distribution in Eq. (12) are the same, namely, that the impurity spins are uncorrelated and are also independent of the $\{K_{i,j}\}$.

## C. Phase diagrams

We now examine the physics contained in Eqs. (14a), (14b), and (17). We first consider the case where $K_0 = 0$; we begin by determining the spin glass transition temperature $T_g$. Expanding the right-hand-side of Eq. (14b) in powers of $q$, we find $T_g$ is determined by

$$1 = \frac{K}{2\pi^2 T_g} \left[\psi'\left(\frac{1}{2} + \frac{T_K}{4\pi T_g}\right)\right], \qquad (18)$$

where $\psi'(z)$ is the trigamma function.[18] For $T_K = 0$, Eq. (18) reduces to $T_g = K/4$, which is the spin glass freezing temperature of the SK model with spin-1/2 impurities. Also, using an asymptotic expansion for $\psi'(z)$, we find that $T_g$ is driven to zero for $K_c = \pi T_K/2$. Turning to Eq. (17) and performing the integral with $q \to 0$, the result is the right-hand-side of Eq. (18). Hence, from Eq. (18) the inequality in Eq. (17) is
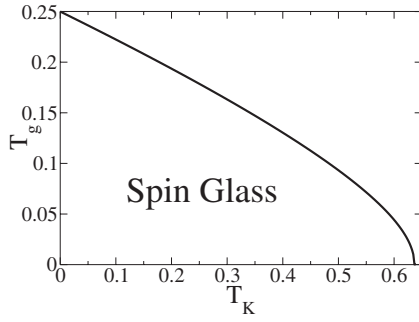
FIG. 2. Phase diagram in the $T_K$-$T_g$ plane (for $K_0=0$) determined from Eq. (18).

never satisfied; the phase described by the field distribution in Eq. (12) is never stable. Therefore, $T_g$ itself marks the transition to a state with broken ergodicity. The spin glass freezing temperature $T_g$ determined from Eq. (18) is shown in Fig. 2.

Now we consider the case where $K_0 \neq 0$. To simplify things a bit, we formally consider the $T \rightarrow 0$ limit. [As noted above, the approach considered in this work is not appropriate to consider the $T \rightarrow 0$ limit. However, we formally consider this limit, as it allows us to understand the competition between $T_K$ and $K_0$ in the simplest context (without the complication of a finite temperature).] By numerically integrating Eqs. (14a), (14b), and (17), we determined the phase diagram in the $K_0$-$T_K$ plane; the results are shown in Fig. 3. We find three distinct phases to arise: a spin glass phase, a ferromagnetic phase, and a "mixed" phase. In the spin glass phase, the spontaneous magnetization vanishes $m=0$, and the inequality in Eq. (17) is violated. In the ferromagnetic phase, $m \neq 0$ but the inequality in Eq. (17) is satisfied. In the mixed phase, $m \neq 0$; the inequality in Eq. (17) is violated as well. Hence, the field distribution is given by Eq. (12) in the ferromagnetic phase, but not in the spin glass and mixed phases. Notice that Eq. (12) is stable over a substantial region in the $K_0$-$T_K$ plane.

## IV. BROKEN ERGODICITY PHASES

Having determined the phase diagram(s) and, in particular, the regimes of stability of Eq. (12), we now determine $\mathcal{P}(h_i)$ in the phases with broken ergodicity. Recall that $\mathcal{P}(h_i)$
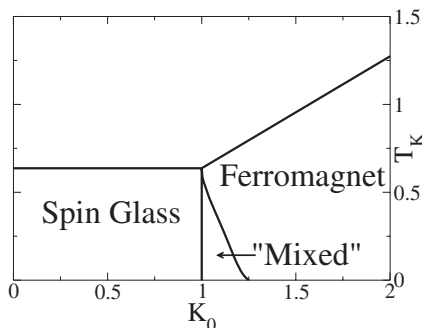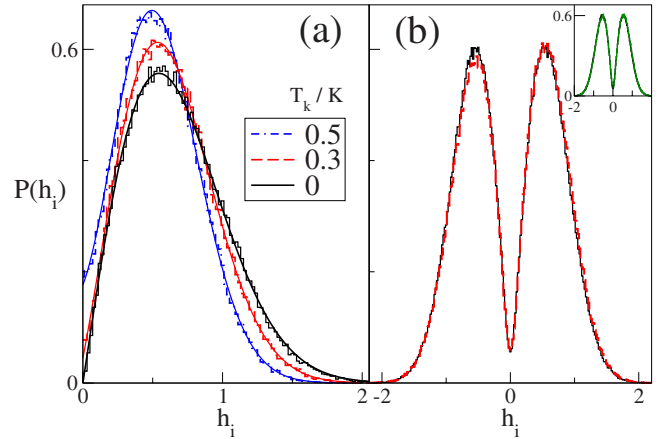


FIG. 3. $T=0$ phase diagram in the $K_0$-$T_K$ plane.



FIG. 4. (Color online) (a) $\mathcal{P}(h_i)$ with $K_0=0$ for various values of $T_K$. (b) $\mathcal{P}(h_i)$ with $T_K/K=0.6$ for various values of $K_0$. Main figure: (black) solid line—$K_0=0$; (red) dashed line—$K_0=1.1$ K. Inset: (black) solid line—$K_0=0$; (green) dashed line—$K_0=0.9$ K.

in Eq. (12) was obtained by assuming the $\{\langle \tau_i^z \rangle\}$ are uncorrelated and independent of the $\{K_{i,j}\}$ As discussed above in Sec. III B, this assumption breaks down in the glass phases—in the glass phases, $\langle \tau_i^z \rangle$ for the $i$th spin must be computed self-consistently, taking into account correlations with all the other $\{\langle \tau_j^z \rangle\} \forall j$. To this end, we perform a "spatially unrestricted mean-field" calculation to determine the $\{\langle \tau_i^z \rangle\}$ and, hence, the $h_i$ in Eq. (5). Using $\langle \tau_i^z \rangle$ in Eq. (13), the $\{h_i\}$ are determined via

$$h_i = \sum_{j \neq i} K_{i,j} \frac{1}{\pi} \text{Im}\left[ \psi\left( \frac{1}{2} + \frac{T_K}{4\pi T} + i\frac{h_j}{2\pi T} \right) \right]. \quad (19)$$

In Eq. (19), we are not considering the contribution from the reaction term. Similar to other works, we have found the reaction term to give severe problems with convergence.[22] It is well known that the mean-field equations without the reaction term overestimates the glass freezing temperature $T_g$;[2,8] properties near the glass transition are not expected to be described correctly. Indeed, Ref. 23 considered a spin-glass model where the reaction term vanishes; it was found that the properties near $T_g$ were different from the SK model. However, both the model considered in Ref. 23 and the SK model were found to have similar properties in the low-temperature phase. In particular, the free enery landscape of both models was very complex with many metastable states. It has been found in conventional spin glasses that the properties within the various phases are described reasonably well when the reaction term is not considered.[24] Hence, Eq. (19) is expected to capture the essential physics of the glass phase.

In Fig. 4, we show results for $\mathcal{P}(h_i)$ determined numerically by Eq. (19) [and Eq. (6)] in the spin glass and mixed phases. The results were generated by considering 1000 impurity spins averaged over 100 realizations of the $\{K_{i,j}\}$. Figure 4(a) shows $\mathcal{P}(h_i)$ at $T=0$ and $K_0=0$ for several values of $T_K$. We see that $\mathcal{P}(h_i)$ has weight shifted from smaller to larger $h_i$, compared to Eq. (12) (with $m=0$). This occurs

TABLE I. $\sigma$, $\lambda_1$, and $\lambda_2$ in Eq. (20) determined by a least-squares fitting procedure for several values of $T_K$.

| $T_K/K$ | $\sigma$ | $\lambda_1$ | $\lambda_2$ |
|---|---|---|---|
| 0.0 | 0.594 | 0.0 | 1.0 |
| 0.3 | 0.427 | 0.052 | 0.562 |
| 0.5 | 0.32 | 0.177 | 0.211 |

because the system lowers its energy when the impurity spins are aligned with the internal fields acting on them [see Eq. (4)]. Moreover, $\mathcal{P}(h_i)$ has a linear suppression for small $h_i$. We found that $\mathcal{P}(h_i)$ in Fig. 4(a) could be fit reasonably well by a function of the form

$$\mathcal{P}(h_i) = \left( \frac{\lambda_1}{\sqrt{\sigma\pi}} + \lambda_2 \frac{|h_i|}{\sigma} + \lambda_3 \frac{2h_i^2}{\sigma\sqrt{\pi\sigma}} \right) \exp(-h_i^2/\sigma), \quad (20)$$

where $\sigma$, $\lambda_1$, and $\lambda_2$ are fitting parameters. ($\lambda_1, \lambda_2 \lesssim 1$; $\lambda_3 = 1 - \lambda_1 - \lambda_2$.) The values of $\sigma$, $\lambda_1$, and $\lambda_2$ determined by a least-squares fitting procedure are given in Table I; the fits to Eq. (20) are shown by solid lines in Fig. 4. Notice that for $T_K = 0$, $\lambda_1 = 0$ and $\lambda_2 = 1$, hence $\mathcal{P}(h_i) \sim |h_i| \exp(-h_i^2/\sigma)$.[14] For $T_K \neq 0$, $\mathcal{P}(h_i)$ has a finite intercept for $h_i \rightarrow 0$, hence $\lambda_1 \neq 0$. This occurs because for $T_K \neq 0$, screening of the impurity spins due to the Kondo effect reduces the effective magnitude of their moments, and hence reduces the effective field they can produce. As a result, the probability for $h_i$ at a site to be zero is increased, compared to the case where $T_K = 0$.

We now consider the case where $K_0 \neq 0$. Figure 4(b) shows results for $\mathcal{P}(h_i)$ at $T=0$ and $T_K = 0.3$ K for several values of $K_0$. Throughout the spin glass phase $K_0 < 1$, there is essentially no change in $\mathcal{P}(h_i)$. Indeed, the inset of Fig. 4(b) shows $\mathcal{P}(h_i)$ for $K_0$ near the boundary between the spin glass and mixed phases, $K_0 = 0.9$ K. For comparison, results for $K_0 = 0$ are also shown; the results are practically identical. The main pannel in Fig. 4(b) shows results for $\mathcal{P}(h_i)$ in the mixed phase. Here, we see that $\mathcal{P}(h_i)$ is similar to the spin glass phase at small $h_i$, namely, there is a linear suppression in $\mathcal{P}(h_i)$. However, while $\mathcal{P}(h_i)$ is symmetric about $h_i = 0$ in the spin glass phase, $\mathcal{P}(h_i)$ is asymmetric in the mixed phase due to the nonzero magnetization.

## V. CONCLUDING REMARKS

To summarize, we discussed the interplay of spin glass physics and the Kondo effect in a model for dilute magnetic alloys. Rather than use the replica formalism, the physics was analyzed in terms of the distribution of internal fields $\mathcal{P}(h_i)$. Utilizing this approach, we determined the phase diagram of the model and, in particular, discussed properties of the glass phase that arises. The approach employed in this work could be utilized/extended to consider an SU(2) invariant interimpurity interaction as well as the Dzyloshinskii-Moriya interaction. Furthermore, this approach should allow one to compute various experimentally measurable quantities.

## ACKNOWLEDGMENTS

[1] A. Hewson, *The Kondo Effect to Heavy Fermions* (Cambridge University Press, Cambridge, 1993).

[2] K. H. Fischer and J. A. Hertz, *Spin Glasses* (Cambridge University Press, Cambridge, 1991).

[3] J. Kondo, Prog. Theor. Phys. **32**, 37 (1964).

[4] M. A. Ruderman and C. Kittel, Phys. Rev. **96**, 99 (1954); T. Kasuya, Prog. Theor. Phys. **16**, 45 (1956); K. Yosida, Phys. Rev. **106**, 893 (1957).

[5] F. Schopfer, C. Bauerle, W. Rabaud, and L. Saminadayar, Phys. Rev. Lett. **90**, 056801 (2003).

[6] A. Theumann, B. Coqblin, S. G. Magalhaes, and A. A. Schmidt, Phys. Rev. B **63**, 054409 (2001); A. M. Sengupta and A. Georges, *ibid.* **52**, 10295 (1995).

[7] O. Parcollet and A. Georges, Phys. Rev. B **59**, 5341 (1999).

[8] D. J. Thouless, P. W. Anderson, and R. G. Palmer, Philos. Mag. **35**, 593 (1977).

[9] V. Barzykin and I. Affleck, Phys. Rev. B **61**, 6170 (2000).

[10] C. C. Chamon and E. Fradkin, Phys. Rev. B **56**, 2012 (1997).

[11] Y.-J. Kao, G. S. Grest, K. Levin, J. Brooke, T. F. Rosenbaum, and G. Aeppli, Phys. Rev. B **64**, 060402(R) (2001).

[12] See, for example, A. O. Gogolin, A. A. Nersesyan, and A. M. Tsvelik, *Bosonization Approach to Strongly Correlated Systems* (Cambridge University Press, Cambridge, 1999).

[13] D. Sherrington and S. Kirkpatrick, Phys. Rev. Lett. **35**, 1972 (1975).

[14] R. G. Palmer and C. M. Pond, J. Phys. F: Met. Phys. **9**, 1451 (1979).

[15] D. Stauffer and K. Binder, Z. Phys. B **34**, 97 (1979).

[16] D. S. Fisher and D. A. Huse, Phys. Rev. Lett. **56**, 1601 (1986).

[17] M. W. Klein, Phys. Rev. B **14**, 5008 (1976).

[18] I. S. Gradshteyn and I. M. Ryzhik, *Table of Integrals, Series, and Products* (Academic Press, San Diego, 1994); M. Abramowitz and I. A. Stegun, *Handbook of Mathematical Functions* (Dover, New York, 1965).

[19] J. R. L. de Almeida and D. J. Thouless, J. Phys. A **11**, 983 (1978).

[20] M. V. Feigelman and A. M. Tsvelik, Zh. Eksp. Teor. Fiz. **77**, 2524 (1979) [Sov. Phys. JETP **50**, 1222 (1980)].

[21] A. Khurana and J. A. Hertz, J. Phys. C **13**, 2715 (1980).

[22] See D. D. Ling, D. R. Bowman, and K. Levin, Phys. Rev. B **28**, 262 (1983), and references therein.

[23] A. Bray, H. Sompolinsky, and C. Yu, J. Phys. C **19**, 6389 (1986).

[24] C. M. Soukoulis, K. Levin, and G. S. Grest, Phys. Rev. B **28**, 1495 (1983).